

Earth Tides: An Introduction

Duncan Carr Agnew

1. Introduction

The motions induced in the solid Earth by tidal forces are known as Earth tides; we examine these in some detail because they are, in any strain or tilt record of reasonable quality, the dominant signal almost all of the time. For borehole instruments they provide the only signal known well enough to be useful for calibration. The Earth tides are much easier to model than the ocean tides because the Earth is more rigid than water, and has a much simpler shape than the ocean basins—which makes the response of the Earth to the tidal forces much easier to find, and much less dependent on details. While this is an advantage if your aim is to compute the Earth tides, it is very much a disadvantage if you want to use Earth-tide measurements to find out something about the Earth. Since Earth tides can be described well with only a few parameters, knowing those few parameters does not provide much information.

1.1. Historical Note

That the tides provide little information on Earth structure helps to explain why Earth-tide studies have recently been a backwater of geophysics—albeit one in which a few of us have enjoyed paddling about. There was a time, between about 1870 and 1930, when not a lot was otherwise known about the inside of the Earth, and Earth tides were central to solid-earth geophysics (Brush 1996). At the start of this period, one assumption was that the Earth was almost entirely molten (based on a reasonable extrapolation of the surface temperature gradient). William Thomson (later Lord Kelvin) pointed out that, if this were so, the Earth would move up and down as much as the ocean would, and the measured tide (the difference of the two motions) would be small compared to the tidal potential—and it isn't. Kelvin knew, of course, that this argument works only for equilibrium tides, and had George Darwin (who we will encounter later in the section on tidal forcing) analyze tide-gauge data for long-period tides in the ocean. These proved to have an amplitude which enabled Kelvin to deduce that if the Earth had a uniform rigidity (shear modulus) this was greater than that of glass and less than that of steel.

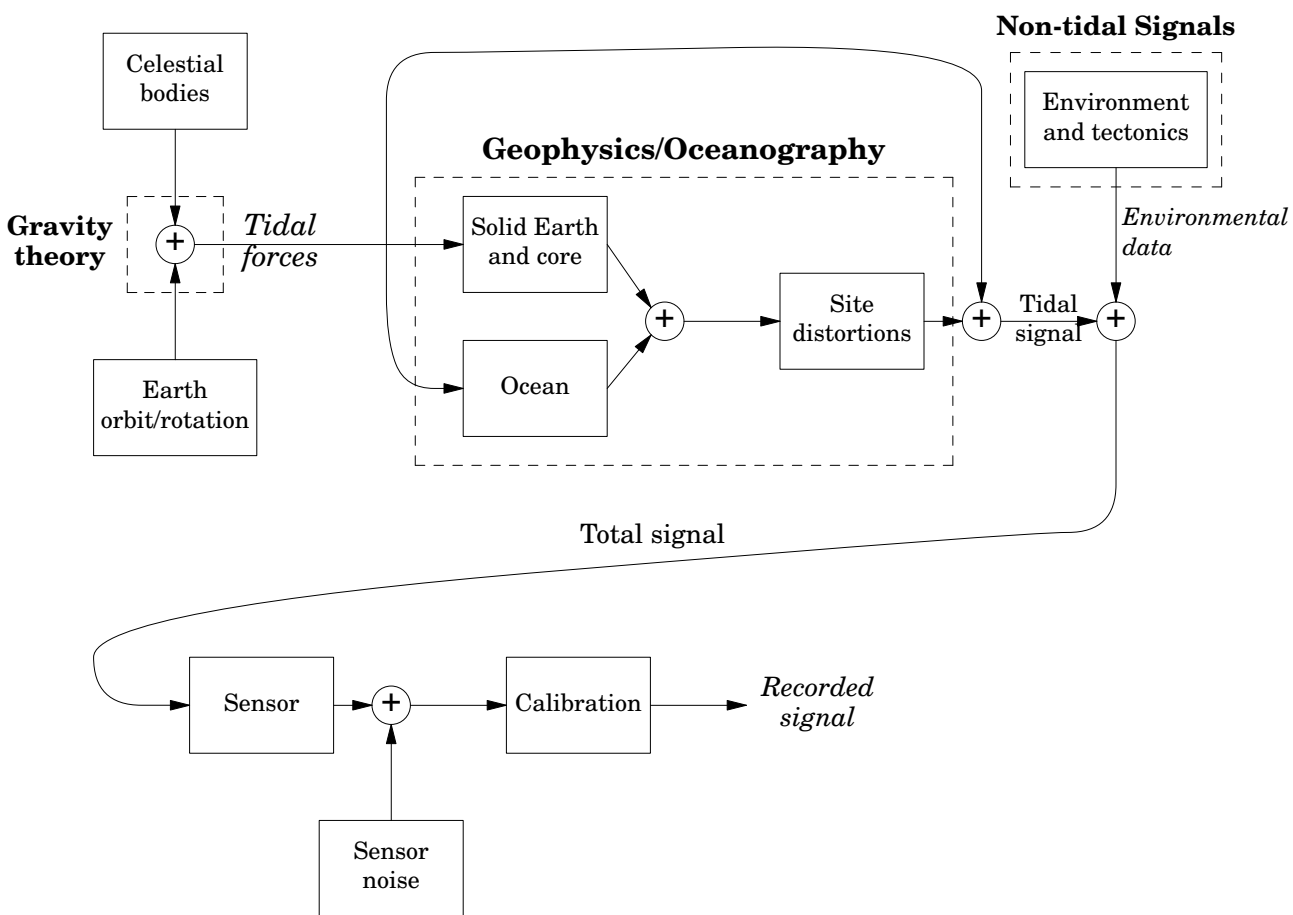
Kelvin and Darwin knew that if the earth deformed tidally this deformation could be measured in the laboratory, and in fact measured for the diurnal and semidiurnal tides, which for the solid Earth are close to equilibrium. This would provide results much more quickly than waiting for the long-period ocean tides to emerge from the noise. At least this was the plan; when George Darwin (with his brother Horace) built a tiltmeter they found so much noise that they concluded that “the measurement of earth tides must remain forever impossible”. But other experimenters (notably Hecker, in Germany) showed this was not so, and from 1890 to 1920 there was a burst of tidal tilt measurements. In retrospect the best were made by A. A. Michelson, who built a miniature ocean at Yerkes Observatory in Wisconsin, in the form of two 150-m tubes (one north-south and one east-west), each half-filled with water. The (very small) tides in these were measured (how else)

interferometrically, and of course for these small bodies of water all the tides were equilibrium. Effectively, the measurement was one of tilt; this was the first longbase tiltmeter. Harold Jeffreys, in 1922, used these data to show that the average rigidity of the Earth was about what Kelvin had found; crucially, this rigidity was much *less* than the average rigidity of the mantle as found by seismology, implying that the core must be of very low rigidity, indeed fluid—the first clear, and generally accepted, demonstration of this fact.

In this determination (the reverse, in some sense, of Kelvin’s) seismology played a major role; and the greater resolving power of seismic waves made it possible to determine far more about Earth structure than could ever be done with tides. This did not mean that people stopped making the measurements (which were technically challenging) but it does not appear, especially in retrospect, that much has come out of it all.

In addition to the need to understand tides for strain measurement, some of the modern revival of interest in this subject has come from the improvements of geodetic measurements: the earth tides are a source of motions that need to be taken into account in modeling these data.

Figure 1.1: An Earth-Tide Flow-Chart



1.2. An Overview

The flow-chart in Figure 1.1 tries to indicate some of what goes into an earth-tide (or ocean-tide) measurement. In this, entries in *italics* represent things we know (or think we do); ones in **boldface** (over the dashed boxes) represent things we can learn about. Though we usually take the tidal forcing to be known, it is of course computed using a particular theory of gravity; and it is actually the case that earth-tide measurements are the best evidence available for general relativity as opposed to some other alternative theories. The large box labeled “Geophysics/Oceanography” includes what we can learn about from the tides; the arrow going around it means that we would see tides (in some quantities) even if the Earth were oceanless and rigid. And, most importantly, measurements made to find out about tides can contain other useful information as well: tide gauges tell us about other oceanographic variations, and methods developed for precise measurements of earth tides can detect other environmental and tectonic signals.

Some terminology may be helpful at this point. The **theoretical tides** are ones that we compute from a set of models; essentially all of earth-tide studies consists of comparing observations with these. The first step is to compute the tidal forcing, or **equilibrium tidal potential**, from the astronomy. From these, we can compute two parts that sum to give the total theoretical tide: the **body tides** are what would be observed on an oceanless but otherwise realistic Earth; the **load tides** come from the effects of the water being moved about.

We look at the tidal forcing first, and in some detail because the nature of this forcing governs how we have to analyze tidal data. We next consider the body tides: how the Earth responds to the tidal forcing, and what effects this produces that we can measure, including tilt and strain. After this come the load tides, completing what we need to know to produce theoretical tides. For observed tides, the main question then is, how to estimate them; so we conclude with a discussion of tidal-analysis methods.

This subject has attracted perhaps more than its share of reviews. Melchior (1983) is the great compendium of the classical side of the subject, but is poorly written and not always up to date; it must be used with caution by the newcomer to the field. It does have an exhaustive bibliography. Harrison (1985) reprints a number of important papers, with very thoughtful commentary. The volume of articles edited by Wilhelm *et al.* (1997) is more up-to-date and a better reflection of the current state of the subject.

2. The Tidal Forces

We begin with the tidal forces, which are those that produce deformations in the Earth and ocean. While there is basically no geophysics in this subject—it is a little bit of gravitational potential theory and a lot of astronomy—we will need to know something about it to understand traditional tidal terminology and the nature of the tidal signal. From the standpoint of the geophysical user, this can all be taken as a completely settled subject—indeed, in some ways too settled. The extraordinarily high accuracy of astronomical theory has tempted a series of workers to produce descriptions of the tides whose precision far exceeds anything we could hope to

measure: in this field, the romance of the next decimal place has exerted a somewhat irrational pull. I will try to resist this temptation.

2.1. The Basics: An Elementary View

While our formal derivation of the tidal forcing will use potential theory, we begin with two elementary arguments using simple mechanics, to clarify some points that often seem confusing. The first is that the tidal forces are directed away from the center of the Earth both beneath the Moon (or Sun), and at the antipode to this point. The easiest demonstration of why this would be so involves a simple thought experiment. Imagine you are in a (very tall) elevator, and someone cuts the cable. Then you and the elevator will fall freely, and it will seem to you that there is no gravity—which is to say that there is no force needed between you and the floor of the elevator to keep you in the same position relative to it: you can float inside it. Now, suppose that the top and bottom of the elevator are separated: someone not only cuts the cable, but removes the walls of the elevator—and you are floating (falling!) between the top and bottom. Since the bottom is closer to the attracting object (say the Earth) than you are, it will experience a slightly greater gravitational force, and accelerate slightly faster than you do, while the top will accelerate slightly less. From your perspective, the top will seem to be pulled up and away from you, and the bottom down and away, just as though there was a force acting away from you, both towards the Earth and away from it. This is, exactly, the tidal force, which just depends on gravity not being the same everywhere.

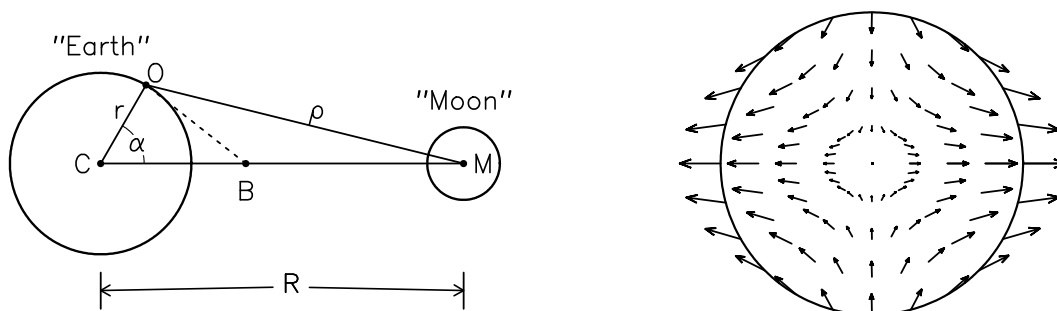


Figure 2.1

Matters are rendered more confusing in the real situation because the motion is along curved orbits. This has led to some confusion about the role of the apparent force experienced on a moving object, usually called the “centrifugal force”. To see where this comes in (or, actually, doesn’t) we consider a simplified situation, shown in the left plot in Figure 2.1. Two bodies (call them the Earth and Moon) orbit about their barycenter B, which for this two-body problem is fixed. (The figure is in the orbital plane). Assume that the Earth rotates at the same rate as it orbits, so that an observation point O is fixed in relation both to C (the center of the Earth) and B (This is in fact true for the Moon). The rate of rotation has angular velocity ω . The point at O experiences a centrifugal force along the line BO, which we can write as

$$\omega^2 \vec{BO} = \omega^2 (\vec{BC} + \vec{CO}) \quad (2.1)$$

where we have simply used the triangle of forces. But an acceleration along \vec{CO} is, in an Earth-fixed reference system, purely radial and unchanging, so we may ignore it. The remaining part, $\omega^2 \vec{BC}$, does change with time, as the direction \vec{BC} changes. But this acceleration is just the opposite to the attraction of the Moon at C, which is what keeps the Earth in orbit around B.

The total force at O, neglecting the unchanging radial part, is thus the attraction of the Moon at O, plus the $\omega^2 \vec{BC}$ part of (1). But this is just equal to the attraction at O minus that at C. The tidal force is thus a differential force, distributed as shown in Figure 2.1 (right). Under the attracting body (which is called the **sub-body point**), and at the antipode of that point, it is oppositely directed in space, though in the same way (up) viewed from the Earth. It is in fact larger at the sub-body point than at its antipode, though if the ratio r/R is small (for Figure 2.1 it is $1/60$) this difference is also small, as we will now derive more formally.

2.2. The Tidal Potential (I)

We now derive the tidal force—or rather, we derive the **tidal potential**, as this turns out to be more useful. If M_a is the mass of the attracting body, the gravitational potential, V_{tot} , from it at O is

$$V_{tot} = \frac{GM_a}{\rho} = \frac{GM_a}{R} \frac{1}{\sqrt{1 + (r/R)^2 - 2(r/R) \cos \alpha}} \quad (2.2)$$

using the cosine rule from trigonometry. Here r is the distance of O from C, ρ the distance from O to M, and α the angular distance between O and the sub-body point of M. We can write the square-root term as a sum of Legendre polynomials, using the generating-function expression for these, which yields

$$V_{tot} = \frac{GM_a}{R} \sum_{n=0}^{\infty} \left(\frac{r}{R}\right)^n P_n(\cos \alpha) \quad (2.3)$$

The $n = 0$ term is constant in space, so its gradient (the force) is zero; it can thus be discarded. The $n = 1$ term is

$$\frac{GM_a}{R^2} r \cos \alpha = \frac{GM_a}{R^2} x \quad (2.4)$$

where x is the Cartesian coordinate along the C-M axis. The gradient of this is a constant, giving a constant force along the direction to M. But this is just the orbital force at C, which we subtract to get the tidal force. Doing the same with the potential, the tidal potential is just (3) with the two lowest terms removed:

$$V_{tid}(t) = \frac{GM_a}{R(t)} \sum_{n=2}^{\infty} \left(\frac{r}{R(t)}\right)^n P_n[\cos \alpha(t)] \quad (2.5)$$

where we have made R and α , as they actually are, functions of time t —which makes V such a function as well.

Now we can put in some numbers for the actual situation. If r is the radius of the Earth, then for the Moon $r/R = 1/60$, so that the importance of terms in the sum (5) decreases fairly rapidly with increasing n ; in practice we need only consider $n = 2$ and $n = 3$, and perhaps $n = 4$ for the highest precision; the $n = 4$ tides are just

detectable in very-low-noise gravimeters. These different values of n are referred to as the **degree- n** tides. For the Sun, $r/R = 1/23,000$, so we need only consider the degree-2 solar tides.

If we look at degree-2, the magnitude of V_{tid} is proportional to GM_a/R^3 . If we normalize this quantity to make the value for the Moon equal to 1, the value for the Sun is 0.46, for Venus $5 \cdot 10^{-5}$, and for Jupiter $6 \cdot 10^{-6}$, everything else being even smaller. To any precision we are likely to need for actual measurements, we need to consider only the **lunisolar** tides—though, as we will see, some expansions of the tidal potential do include planetary tides.¹

2.3. The Tidal Potential (II)

Further understanding of the tidal forces comes if we put the expressions into geographical coordinates rather than distance from the sub-body point. Suppose our observation point O is at colatitude θ and east longitude ϕ (which is fixed) and that the sub-body point of M is at colatitude $\theta'(t)$ and east longitude $\phi'(t)$. Then we may apply the addition theorem for spherical harmonics to get, instead of (5),

$$V_{tid} = \frac{GM_a}{R(t)} \sum_{n=2}^{\infty} \left(\frac{r}{R(t)} \right)^n \frac{4\pi}{2n+1} \sum_{m=-n}^n Y_{nm}^*(\theta'(t), \phi'(t)) Y_{nm}(\theta, \phi) \quad (2.6)$$

where we have used the fully normalized complex spherical harmonics defined by

$$Y_{nm}(\theta, \phi) = N_n^m P_n^m(\cos \theta) e^{im\phi} \quad (2.7)$$

where N_n^m is the normalizing factor

$$N_n^m = (-1)^m \left[\frac{2n+1}{4\pi} \frac{(n-m)!}{(n+m)!} \right]^{\frac{1}{2}} \quad (2.8)$$

and P_n^m is the associated Legendre polynomial of degree n and order m , as given in Munk and Cartwright (1966). As is true for any part of geophysics that employs spherical harmonics, it is important to be aware of other possible normalizations.

To make the tidal potential more meaningful we express it as V_{tid}/g , where g is the Earth's gravitational acceleration; this has the dimension of length, and can easily be interpreted as the change in elevation of the geoid, or of an equilibrium surface such as an ideal ocean. (Hence its name, the **equilibrium potential**). If, as is conventional, g is taken to have its value on the Earth's equatorial radius r_{eq} , and r is held fixed at that radius in (6), we get

$$\begin{aligned} \frac{V_{tid}}{g} &= r_{eq} \frac{M_a}{M_{\oplus}} \sum_{n=2}^{\infty} \frac{4\pi}{2n+1} \left(\frac{r_{eq}}{R} \right)^{n+1} \sum_{m=-n}^n Y_{nm}^*(\theta', \phi') Y_{nm}(\theta, \phi) \\ &= \sum_{n=2}^{\infty} K_n \zeta^{n+1} \frac{4\pi}{2n+1} \sum_{m=-n}^n Y_{nm}^*(\theta', \phi') Y_{nm}(\theta, \phi) \end{aligned} \quad (2.9)$$

¹ At very high precision, we also need to consider also another small effect, namely that the acceleration of the Earth is not exactly that given by a potential of form (4). This would be true for a spherically symmetric Earth; for the real Earth, the C_{20} term in the gravitational potential, makes the acceleration of the Moon by the Earth (and vice-versa) depend on more than just (4). The resulting tides are however small.

where the constant K includes all the physical quantities:

$$K_n = r_{eq} \frac{M_a}{M_\oplus} \left(\frac{r_{eq}}{\bar{R}} \right)^{n+1} \quad (2.10)$$

where M_\oplus is the mass of the Earth and \bar{R} is the mean distance of the body; the quantity $\xi = \bar{R}/R$ expresses the normalized change in distance. For the Moon, K_2 is 0.35837 m, and for the Sun, 0.16458 m.

In both (6) and (9), we have been thinking of θ and ϕ as giving the location of a particular place of observation; but if we consider them to be variables, the $Y_{nm}(\theta, \phi)$ describes the geographical distribution of V/g on the Earth. The time-dependence of the tidal potential comes from time variations in R and θ' , which vary relatively slowly because of the orbital motion of M around the Earth; ϕ' varies much more rapidly as the Earth rotates beneath M.² The second sum in (9) thus separates the tidal potential of degree n into parts, called **tidal species**, that vary with frequencies around 0, 1, 2, ... n times per day; for the largest tides (n , the degree, being 2), there are three such species, with names and latitude dependences given in Table 1.

Table 1: Main Tidal Species in the Potential

| m | Name | Colatitude dependence of V_{tid}/g |
|-----|-------------|--------------------------------------|
| 0 | Long-period | $3 \cos^2 \theta - 1$ |
| 1 | Diurnal | $3 \sin \theta \cos \theta$ |
| 2 | Semidiurnal | $3 \sin^2 \theta$ |

The diurnal tidal potential is largest at mid-latitudes and vanishes at the equator; the semidiurnal part is largest at the equator; both vanish at the poles, where the long-period is largest. (As we will see, this does not exactly carry over to the strain tides, which depend on surface gradients of the potential).

To proceed beyond this it is desirable to separate the time-dependent and space-dependent parts a bit more explicitly. We adopt the approach of Cartwright and Taylor (1971) who produced what was for a long time the standard harmonic expansion of the tidal potential. We can write (9) as

$$\begin{aligned} \frac{V_{tid}}{g} &= \sum_{n=2}^{\infty} K_n \xi^{n+1} \frac{4\pi}{2n+1} \left[Y_{n0}(\theta', \phi') Y_{n0}(\theta, \phi) + \sum_{m=1}^n Y_{n-m}^*(\theta', \phi') Y_{n-m}(\theta, \phi) + Y_{nm}^*(\theta', \phi') Y_{nm}(\theta, \phi) \right] \\ &= \sum_{n=2}^{\infty} K_n \xi^{n+1} \frac{4\pi}{2n+1} \left[Y_{n0}(\theta', \phi') Y_{n0}(\theta, \phi) + \sum_{m=1}^n 2 \operatorname{Re} [Y_{nm}^*(\theta', \phi') Y_{nm}(\theta, \phi)] \right] \end{aligned}$$

Now define complex (and time-varying) coefficients $T_{nm}(t) = a_n^m(t) + ib_n^m(t)$ such that

$$\frac{V_{tid}}{g} = \operatorname{Re} \left[\sum_{n=2}^{\infty} \sum_{m=1}^n T_{nm}^*(t) Y_{nm}(\theta, \phi) \right] \quad (2.11)$$

and we find that these coefficients are, for $m = 0$,

² If you think this sounds like an Earth-centered description of what is happening, you are correct—for this application a geocentric approach is perfectly correct, and often more clear.

$$T_{n0} = \left(\frac{4\pi r_{eq}}{2n+1} \right)^{\frac{1}{2}} K_n \xi^{n+1} P_n^0(\cos \theta') \quad (12a)$$

and, for $m \neq 0$

$$T_{nm} = (-1)^m \frac{8\pi}{2n+1} K_n \xi^{n+1} N_n^m P_n^m(\theta') e^{i\phi'} \quad (12b)$$

from which we can find the real-valued, time-varying quantities $a_n^m(t)$ and $b_n^m(t)$, which we will use below in computing the response of the Earth.

2.4. Computing the Tides (I): Direct Computation

Equations (11) and (12) suggest a straightforward way to compute the tidal potential (or, as we will see, other theoretical tides), by finding the T_{nm} as a function of time. This is to use an **ephemeris** for the Sun and Moon (and the other planets if we wish): that is, a description of the location of these bodies in celestial coordinates. By including the rotation of the Earth, we can convert these positions to the coordinates of the sub-body point, θ' and ϕ' and the distance R , and then use equation (12). Once we have the T_{nm} , we can combine these with the spatial factors in (11) to get $\frac{V_{tid}}{g}$, either for a specific location or as a distribution over the whole Earth. As we will see below, this formulation carries over with only minor modifications to the various geophysical quantities, including tilt and strain. And, these modifications involve no changes to the T_{nm} : we need to do the astronomy only once.

Such a direct computation also has the advantage, compared with the harmonic methods to be discussed in the next section, of having an accuracy limited only by that of the ephemeris. If we take derivatives of (12) with respect to R , θ' and ϕ' , we find that relative errors of 10^{-4} in V_{tid}/g would be caused by errors of 7×10^{-5} rad ($14''$) in θ' and ϕ' , and 3×10^{-5} in ξ . (We pick this level of error because, as we will see below, it is much less than the errors in finding tidal constants of strain data, given typical noise levels.) Note that the errors in the angular quantities correspond to errors of about 400 m in the location of the sub-body point, so our model of Earth rotation, and our station location, needs to be good to this level. This might not seem very onerous, but note that it requires 1 second accuracy in the timing of the data.

There are two types of ephemerides available. An **analytical** ephemeris is a closed-form algebraic description of the motion of the body as a function of time. Obviously this can be converted directly into computer code. The most precise ephemerides are **numerical**, coming from numerical integration of the equations of motion, with parameters chosen to best fit some set of observational data. While such direct integration is now standard (in, for example, the estimation of GPS satellite orbits), it was not practical until the 1960's—and it remains a specialized area, even within celestial mechanics. For routine computation it also poses the difficulty that the results are available only as tables, not necessarily covering the time of interest.

The first tidal-computation program based directly on an astronomical ephemeris was that of Longman (1959), still in use for making rough tidal

corrections for gravity surveys. Longman's program, like some others, computed accelerations directly, thus somewhat obscuring the utility of an ephemeris-based approach to all tidal computations. Munk and Cartwright (1966) developed this method for the tidal potential (it is their treatment that has been followed here), though (like Longman) using a fairly simplified lunar ephemeris. Subsequent programs such as that of Harrison (1971), incorporated into the `ertid` routine distributed with the PIASD and SPOTL packages, and Tamura (1982) used a subset of the lunar theory of Brown, as did the more precise program of Broucke, Zurn, and Slichter (1972). Merriam (1992) used even more precise ephemerides.

Numerical ephemerides have been used primarily to produce reference time series, rather than for general-purpose programs. Most (e.g., Hartmann and Wenzel 1995) have relied on the solar system ephemerides produced by JPL. The main purpose has been to use these series as the basis for a harmonic expansion of the tidal potential, a standard method to which we now turn.

2.5. Computing the Tides (II): Harmonic Decompositions

Since the work of Thomson and Darwin in the 1870's and 1880's, the most common method of analyzing and predicting the tides, and of expressing tidal behavior, has been through a **harmonic expansion** of the tidal potential. In this, we express the T_{nm} as a sum of sinusoids, whose frequencies are related to combinations of astronomical frequencies and whose amplitudes are determined from the expressions in the ephemerides for R , θ' , and θ . In such an expansion, we write the complex T_{nm} 's as

$$T_{nm}(t) = \sum_{k=1}^{K_{nm}} A_{knm} e^{i(2\pi f_{knm}t + \phi_{knm})} \quad (2.13)$$

where we sum K_{nm} sinusoids with specified amplitudes, frequencies, and phases, for each degree and order. The individual sinusoids, or harmonics, are called **tidal constituents**.

This method has the advantage that once a table of constituent amplitudes has been produced it remains valid for a long time. What this also does (implicitly) is to make results appear in the frequency domain, something as useful here as in other parts of geophysics. In particular, we can use the same frequencies for any other tidal phenomenon, provided that it comes from a linear response to the driving potential—which is essentially true for the Earth tides. So, while such an expansion was first used for ocean tides (for which it remains the standard) it works just as well for Earth tides of any type.

We can get the flavor of this approach, and also introduce much important terminology, by finding the tides from the simplest possible representation of the ephemerides. We assume that the Sun and the Moon move in the same way: in a circular orbit around the Earth, with the orbital plane inclined at an angle ε to the Earth's equator. We further assume that the speed in the orbit is constant, with the angular distance from the ascending node (where the orbit plane and the equatorial plane intersect) being βt . (This is called the celestial longitude). Finally, we assume that the rotation of the Earth causes the terrestrial longitude of the ascending node

(fixed in space) to be Ωt ; Ω is the angular speed of the Earth relative to the ascending node (1 revolution per sidereal day). For simplicity, we set the phases to be such that at $t = 0$ the body is at the ascending node and longitude 0° is under it. Finally, we take just the real part of (9), and ignore factors of magnitude 1 (we do not worry about signs).

With these simplifications we consider first the diurnal degree-2 tides ($n = 2, m = 1$). After some tedious spherical trigonometry and algebra, we find that for each body,

$$V/g = K_A \left(\frac{6\pi}{5} \right) \left[\sin \varepsilon \cos \varepsilon \sin \Omega t + \frac{1}{2} \sin \varepsilon (1 + \cos \varepsilon) \sin(\Omega - 2\beta)t + \frac{1}{2} \sin \varepsilon (1 - \cos \varepsilon) \sin(\Omega + 2\beta)t \right]$$

This gives a harmonic decomposition of three constituents for each body, with arguments (of time) Ω , $\Omega - 2\beta$, and $\Omega + 2\beta$; their amplitudes depend on ε , the inclination of the orbital plane. If this were zero, there would be no diurnal tides at all. In practice, we can take it to be 23.44° , the inclination of the Sun's orbital plane (this plane is called the ecliptic). This angle is also the mean inclination of the Moon's orbit—more on this below. This produces the constituents given in Table 2.

Table 2: Diurnal Tides (Simple Model)

| Argument | Moon | | Sun | |
|-------------------|----------------|-------------|----------------|-------------|
| | Freq. (cpd) | Amp. (m) | Freq. (cpd) | Amp. (m) |
| Ω | 1.002738 | 0.254 | 1.002738 | 0.117 |
| $\Omega - 2\beta$ | 0.929536 | 0.265 | 0.997262 | 0.122 |
| $\Omega + 2\beta$ | 1.075940 | 0.011 | 1.008214 | 0.005 |

Here the frequencies are given in cycles per day (cpd). Both the Moon and Sun produce a constituent at 1 cycle per sidereal day. For the Moon, β corresponds to a period of 27.32 days, and for the Sun 365.242 days (one year), so the other constituents are at ± 2 cycles per month, or ± 2 cycles per year, from this. Note that there is *not* a constituent at 1 cycle per lunar (or solar) day—while this may seem odd, it is not unexpected given the degree-2 nature of the tidal potential.

It is convenient to have a shorthand way of referring to these constituents; unfortunately the standard naming system, now totally entrenched, was begun by Thomson for a few tides, and then extended by Darwin in a somewhat *ad hoc* manner. The result is a series of conventional names that simply have to be learned as is (though only the ones for the largest tides are really important). For the Moon, the three constituents have the **Darwin symbols** K_1 , O_1 , and OO_1 ; for the Sun they are K_1 (again, since this has the same frequency for any body), P_1 and ψ_1 .

Next we consider the $m = 2$ case, for which

$$V/g = K_A \left(\frac{24\pi}{5} \right) \left[(1 - \cos^2 \varepsilon) \cos 2\Omega t + \frac{1}{2} (1 + \cos \varepsilon)^2 \cos(2\Omega - 2\beta)t \right]$$

$$+ \frac{1}{2} (1 - \cos \varepsilon)^2 \cos(2\Omega + 2\beta)t \Big]$$

and so again we have three constituents, though the third one, for ε equal to 23.44° , is very small. Ignoring this one, we get the results in Table 3, with three distinct constituents.

Table 3: Semidiurnal Tides (Simple Model)

| Argument | Moon | | Sun | |
|--------------------|----------------|-------------|----------------|-------------|
| | Freq. (cpd) | Amp. (m) | Freq. (cpd) | Amp. (m) |
| 2Ω | 2.005476 | 0.0.055 | 2.005476 | 0.025 |
| $2\Omega - 2\beta$ | 1.932274 | 0.640 | 2.00000 | 0.294 |

The Darwin symbol for the first argument is K_2 ; again, this frequency is the same for the Sun and the Moon, so these combine to make a lunisolar tide. The second argument gives the largest tides: for the Moon, M_2 (for the Moon) or S_2 (for the Sun), at precisely 2 cycles per lunar (or solar) day respectively.

Finally, the $m = 0$, or long-period, case has a constituent at zero frequency (the so-called **permanent tide**), and another with an argument of 2β , making constituents with frequencies of 2 cycles/month (Mf , the fortnightly tide, for the Moon) or 2 cycles per year (Ssa , the semiannual tide, for the Sun). The permanent tide is usually removed from calculations of the theoretical tide used for tidal analysis.

This simple model also demonstrates one other attribute of the tides that becomes very important for an analysis scheme. The amplitudes of all the tidal constituents depend on the orbital inclination ε . For the Sun this quantity (the obliquity of the ecliptic) is nearly invariant (though very slowly decreasing). For the Moon it varies by $\pm 5.13^\circ$ from the obliquity, with a period of 18.61 years. All the lunar tides thus show a periodic variation in amplitude, known as the **nodal modulation**.³ Our simple expressions above show that the resulting variation in M_2 is about $\pm 3\%$, but for O_1 it is for $\pm 18\%$. We can represent such a modulated sinusoid with an expression of the form $\cos \omega_0 t (1 + A \cos \omega_m t)$, with $\omega_0 \gg \omega_m$; this can be shown to be the same as

$$\cos \omega_0 t + \frac{1}{2} A \cos[(\omega_0 + \omega_m)t] + \frac{1}{2} A \cos[(\omega_0 - \omega_m)t]$$

which is to say that we can represent this modulation, in a purely harmonic development, through three constituents, one at the central frequency and two smaller ones (called **satellite constituents**) separated from this by 1 cycle in 18.61 years.

The next level of complication beyond our simple ephemeris would include the ellipticity of the orbits, and all the periodic variations in ε and other orbital parameters. This leads to a great many constituents. The first such expansion, including satellite constituents, was by Doodson (1921), done algebraically from an analytical ephemeris; the result had 378 constituents. Doodson needed a nomenclature for these tides, and introduced one that relies on the fact that, as our simple ephemeris suggests, the frequency of any constituent is the sum of multiples of a few basic

³ The reason for this name is that the change in ε come from the motion of the line of intersection of the Moon's orbital plane with the Sun's orbital plane; this is the line of nodes.

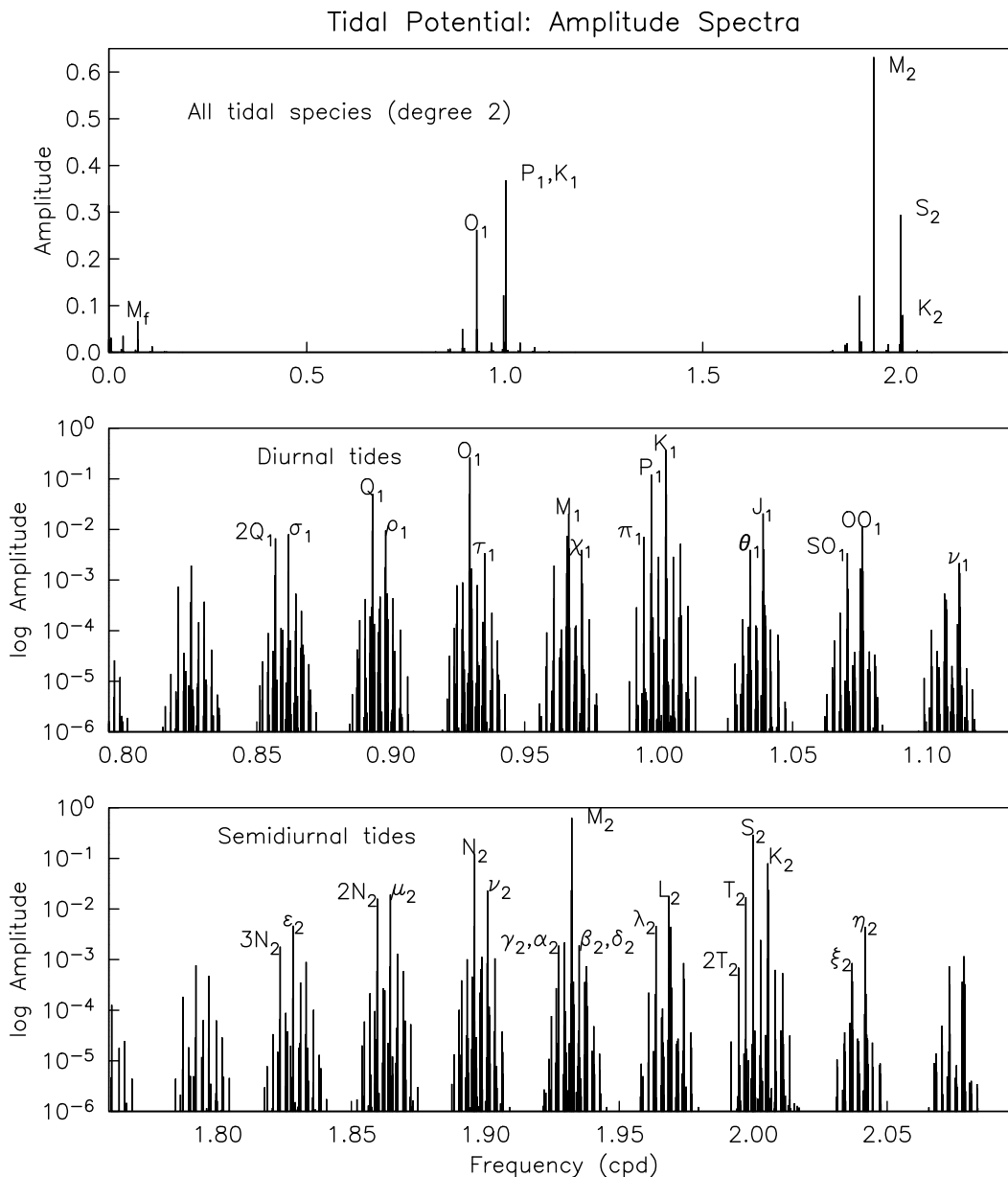


Figure 2.2

frequencies. In practice, we can write the argument of the exponent in (11) as

$$\omega_k t + \phi_k = \left(\sum_{l=1}^6 D_{lk} \omega_l \right) t + \sum_{l=1}^6 D_{lk} \phi_l \tag{2.14}$$

where the ω_l 's are the frequencies corresponding to various astronomical periods, and the ϕ_l 's are the phases of these at some suitable epoch; Table 4 gives a list.⁴ The $l = 1$ frequency is chosen to be one cycle per lunar day exactly, so for the M_2 tide the D_l 's are 2,0,0,0,0. This makes the solar tide, S_2 , have the D_l 's 2,2,-2,0,0. In

⁴Recent tabulations extend this notation with up to five more arguments to describe the motions of the planets. As the tides from these are small we ignore them here.

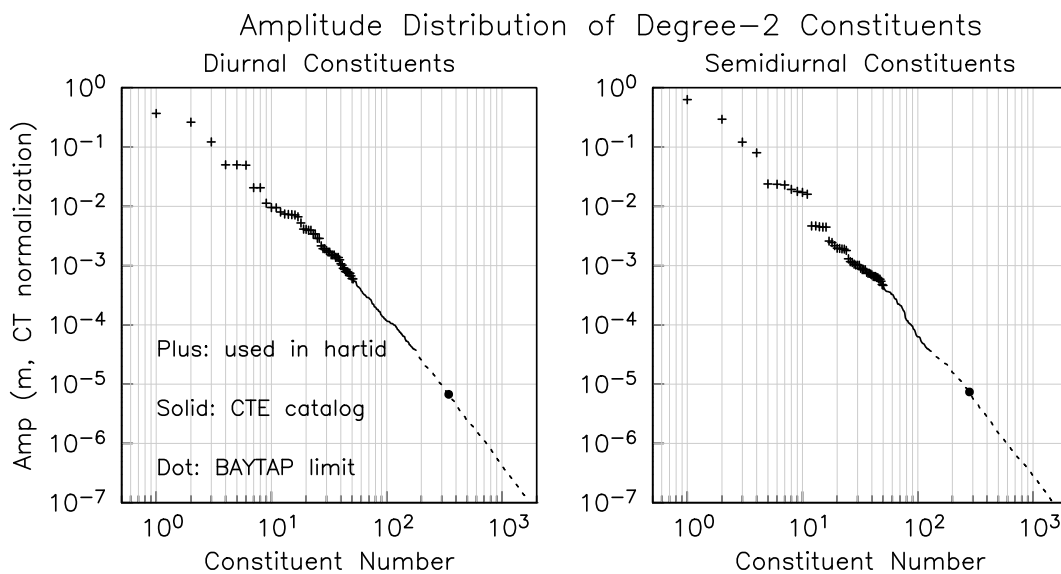
practice, all but the smallest tides have D_{lk} ranging from -5 to 5 for l greater than one; Doodson therefore added 5 to these numbers to make a compact code, so that M_2 becomes 255-555 and S_2 273-555. This is called the **Doodson Number**; the numbers without 5 added are sometimes called Cartwright-Tayler codes.

Table 4: Fundamental Tidal Frequencies

| l | Frequency (cycles/day) | Period | What |
|-----|---------------------------|--------------------|----------------------------------|
| 1 | 0.9661368 | $24^h 50^m 28.3^s$ | Lunar day |
| 2 | 0.0366011 | 27.3216^d | Moon's longitude: tropical month |
| 3 | 0.0027379 | 365.2422^d | Sun's longitude: solar year |
| 4 | 0.0003095 | 8.847^y | Lunar perigee |
| 5 | 0.0001471 | 18.613^y | Lunar nodes |
| 6 | 0.0000001 | 20941^y | Solar perigee |

“Longitude” refers to celestial longitude, measured along the ecliptic.

Figure 2.2 shows the full spectrum of amplitude coefficients actually for the recent expansion of Hartmann and Wenzel 1995). The top panel shows all constituents on a linear scale, making clear that only a few are large, and the separation into different **species** around 0, 1, and 2 cycles/day: these are referred to as the **long-period**, **diurnal**, and **semidiurnal** tidal bands. The two lower panels show an expanded view of the constituents in the diurnal and semidiurnal bands, using a log scale of amplitude to include the smaller constituents. What is apparent from these is that each tidal species is split into a set of bands, separated by one cycle/month; these are referred to as **groups**. Further splitting at smaller frequencies is also apparent; on this scale the nodal modulation is visible only as a thickening of some of the lines. As we will see, all this fine-scale structure poses a challenge to tidal analysis methods.



Since Doodson's rather heroic effort provided the tidal potential to more than adequate accuracy for studying ocean tides, further developments did not take place for the next 50 years, until Cartwright and Tayler (1971) revisited the subject. They computed the potential, using (9), from a more modern lunar ephemeris, and then used special Fourier methods to analyze, numerically, the resulting series, and get amplitudes for the various constituents. The result was a compendium of 505 constituents, which (with errors corrected by Cartwright and Edden 1973) soon became the standard under the usual name of the CTE representation.⁵

As mentioned above, there have been a number of more extensive computations of the tidal potential and its harmonic decomposition, driven by the very high precision available from the ephemerides, the relative straightforwardness of the problem, and (perhaps) the need for more precision for analyzing some tidal data (gravity tides from superconducting gravimeters). Particular expansions are those of Bullesfeld (1985), Tamura (1987), Xi (1987), Hartmann and Wenzel (1995) and Roosbeek (1995). The latest is that of Kudryavtsev (2004), with 27,000 constituents. Figure 2.3 shows the amplitude versus number of constituents for different expansions (including that used in the PIASD program *hartid*); clearly, to get very high accuracy demands a very large number. But not many are needed for a pretty good approximation; and one important result of these efforts is to show that the CTE expansion is good to about 0.1% of the tide in the time domain—and for the analysis of anything but the lowest-noise gravity-tide data, this is quite adequate (we will discuss this further in the notes on power spectra).

2.6. Radiational Tides

A harmonic treatment can also be useful for the various phenomena associated with solar heating, whether temperature effects on the instrument, thermoelastic strains induced in the ground, or the atmospheric tides (thermally induced). The actual heating is usually complicated, but a first approximation makes it proportional to the cosine of the Sun's elevation during the day, and of course zero at night. This asymmetry produces constituents of degree 1 and 2; these have been tabulated by Cartwright and Tayler (1971) and are shown in Figure 2.4 as crosses (for both degrees), along with the tidal potential constituents shown as in Figure 4. The unit for the radiational tides is S , the solar constant. The expanded scale allows us to add a few more Darwin symbols.

That some of these thermal tidal lines coincide with lines in the tidal potential poses a real difficulty for precise analysis of the latter. Strictly speaking, if we have the sum of two constituents with the same frequency, it will be impossible to tell how much each part contributes. The only way to resolve this is to make additional assumptions about how the response to these behaves at other frequencies. Even when this is done, there is a strong likelihood that estimates of these tides will have large systematic errors—which is why, for example, the large K_1 tide is not used in estimating borehole strainmeter coupling, the smaller O_1 tide being used instead.

⁵ A few small constituents at the edges of each band, included by Doodson but omitted by Cartwright, are sometimes added to make a CTED list.

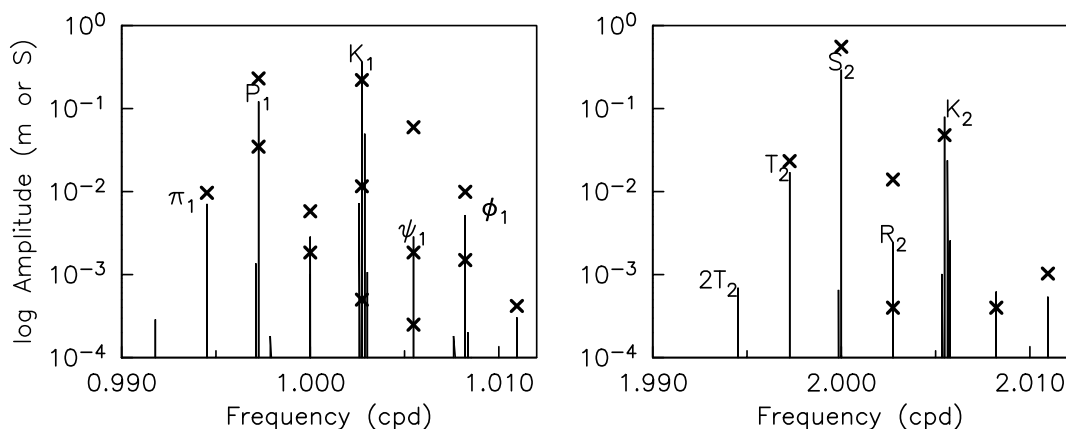


Figure 2.4

3. Tidal Response of the Solid Earth

For most purposes, the tidal response of the Earth is found assuming that it is SNREIO. This ungainly acronym (borrowed and extended from normal-mode seismology) stands for an Earth which is **S**pherical, **N**on-Rotating, **E**lastic, **I**sotropic, and (most important) **O**ceanless. Note that Spherical means completely spherically symmetric, and Isotropic means that the Elasticity is the same in all directions at each point. However, variation in the elastic properties with depth is allowed; otherwise we would have to add, **H**omogeneous.

In addition to these restrictions on the Earth model, we add one more about the tidal forcing: that it has a much longer period than any normal modes of oscillation of the Earth so that we can use a quasi-static theory, taking the response to be an equilibrium one. This is in fact an excellent approximation, since the longest-period normal modes for such an Earth have periods of an hour or less (with one exception to be noted). This is in strong distinction to the situation for the oceans, which have barotropic modes of oscillation with periods close to the diurnal and semidiurnal tidal bands (sometimes, as in the Bay of Fundy, very close indeed).

With all these restrictions and simplifications, the Earth's response to the tidal potential becomes very simple to describe, though not to compute. If the potential is of degree n (the order m does not matter in this case), and at some surface location is V , with potential height V/g , then the distortion of the Earth caused by tidal forces produces an additional gravitational potential $k_n V$, a vertical (that is, radial) displacement $h_n V/g$, and a horizontal displacement $l_n (\nabla V/g)$. These dimensionless quantities are **Love numbers**, after A. E. H. Love (though the parameter l was actually developed by T. Shida). For a standard modern earth model (PREM) $h_2 = 0.6032$, $k_2 = 0.2980$, and $l_2 = 0.0839$. (For comparison, the values for the much older Gutenberg-Bullen earth model are 0.6114, 0.3040, and 0.0832—not very different).

The classical goal of Earth-tide studies was to measure Earth tides and from such measurements deduce the Love numbers and from them Earth structure. As noted above, after some successes this program was overtaken by seismology (not that this seems to have stopped its practitioners), because the values of the Love

numbers are actually quite insensitive to Earth structure. At present it is more common to take the Love numbers to be known and use them to predict an observable (for example, displacement). Such predictions, to be made with full precision, have to allow for the Earth not being SNREIO, which produces modifications. In increasing order of importance these are:

1. The ellipticity of the Earth means that the response to forcing of degree n includes other spherical harmonics; while for a time this was thought to imply a large latitude dependence in the Love numbers, this is not true—but there is an effect of order 10^{-3} .
2. The mantle is only imperfectly elastic (finite Q). This has two effects on the Love numbers; they become complex (small imaginary parts) and because of dispersion they have different values with frequency (and so the tidal values are different from the values appropriate for seismic frequencies).
3. The Earth's ellipticity extends to the core-mantle boundary, and as such allows a free-oscillation mode in which the fluid core (restrained by pressure forces) and solid mantle precess around each other (this is an effect both of the ellipticity and the rotation). This mode of oscillation is known as the Nearly Diurnal Free Wobble or Free Core Nutation. It is not large itself, but it does produce a frequency-dependence in the Love numbers near 1 cycle/day. It also affects the Earth's response to the tidal torques that cause astronomical precession and nutation, and indeed can best be measured astronomically. Measurements of the period of this resonance, both in the Earth tides and in the nutation, suggest that the ellipticity of the core-mantle boundary departs measurably from what would be expected in a hydrostatic Earth: a deep-earth result from astronomical data, which seems to be explicable as distortion of the core-mantle boundary by mantle convection.
4. The most important departure from SNREIO is that the real Earth has oceans, and these respond, in complicated ways, to the tidal potential. The resulting motions and deformations of the solid Earth are called **load tides**; given both their importance and their complexity, we discuss them in detail in a separate section.

3.1. Some Combinations of Love Numbers (I): Gravity and Tilt

Of course, the change in the potential is not measurable; and prior to the development of space geodesy, neither were the vertical or horizontal motions. What could be observed was the ocean tides, tilt, changes in gravity, and local deformation (strain), each of which possesses its own expression in terms of Love numbers. We now derive some of these. We start with the two “classical” earth-tide quantities, gravity and tilt. These both have the feature, unshared with any other earth tide, that they would exist even if the Earth were perfectly rigid. It is therefore standard to express these tides in terms of a ratio to the rigid-earth tides, an approach fairly embedded in the literature, even though it is inapplicable to displacement or strain.

To start, consider the tidal tilts. Since tilt is just the slope of the potential, it scales in the same way that the potential itself does; so the expression for tilt and for

the equilibrium ocean tide is the same. The total tide-raising potential height is $(1 + k_n)V/g$, but the solid earth (on which a tide gauge sits) goes up by $h_n V/g$, so the effective tide-raising potential is $(1 + k_n - h_n)V/g$, sometimes written as $\gamma_n V/g$, with γ_n being called the **diminishing factor** to be applied to the tide-raising potential. For the PREM model it is 0.6947: not a small correction.

The effect of tides on measured gravity was, prior to space geodesy, the most often measured tidal effect. For this, we need to include the radial dependence of the potential. Using a for the local surface radius, the tidal potential is, for tides of degree n ,

$$V_n \left(\frac{r}{a} \right)^n + k_n V_n \left(\frac{a}{r} \right)^{n+1} \quad (3.1)$$

where the first term is the potential caused by the tidal forcing (and for which we have absorbed all non-radial dependence into V_n), and the second is the additional potential induced by the Earth's deformation. The corresponding change in local gravitational acceleration is the radial derivative of the potential:⁶

$$\frac{\partial}{\partial r} \left[V_n \left\{ \left(\frac{r}{a} \right)^n + k_n \left(\frac{a}{r} \right)^{n+1} \right\} \right]_{r=a} = V_n \left[\frac{n}{a} - (n+1) \frac{k_n}{a} \right] \quad (3.2)$$

In addition to this change in gravity from the change in the potential, there is a change in g from the gravimeter being moved up by an amount $h_n V_n/g$. This displacement is multiplied by the gradient of g to get the gravity change. To get the gradient, remember that $g = GM/r^2$ for $r = a$; we then have

$$\frac{\partial g}{\partial r} = \frac{-\partial}{\partial r} \left[\frac{GM}{a^2} \left(\frac{a}{r} \right)^2 \right]_{r=a} = \frac{2g}{a} \quad (3.3)$$

where we have adopted the earth-tide convention that a decrease in g is positive (ground up). Combining this with (2) we get that the change in g is

$$V_n \left[\frac{n}{a} - \left(\frac{n+1}{a} \right) k_n + \frac{2h_n}{a} \right] = \frac{nV_n}{a} \left[1 - \left(\frac{n+1}{n} \right) k_n + \frac{2}{n} h_n \right] \quad (3.4)$$

The nV_n/a is the tidal change in g that would be observed on a rigid Earth (for which h and k are zero); the term which this is multiplied by, namely

$$1 + \frac{2}{n} h_n - \left(\frac{n+1}{n} \right) k_n \quad (3.5)$$

is often written as δ_n and called the **gravimetric factor**. For the PREM model and the degree-2 tides, $\delta_2 = 1.1563$: the gravity tides are only about 16% larger than they would be on a completely rigid Earth, so that most of the tidal gravity signal shows only that the Moon and Sun exist, while giving no information about the Earth.

⁶ Actually, not quite. Gravimeters are always set up to measure along the local vertical, which is not the radius vector, but (very nearly) the normal to the ellipsoid. It was taking gravity to be measured along the radius vector that produced the apparent large latitude effect.

3.2. Combinations of Love Numbers (II): Strain Tides

Again considering the tidal potential of degree n , the displacements at the surface of the Earth ($r = a$) will be, in spherical coordinates,

$$u_r = \frac{h_n V}{g} \quad u_\theta = \frac{l_n}{g} \frac{\partial V}{\partial \theta} \quad u_\phi = \frac{l_n}{g \sin \theta} \frac{\partial V}{\partial \phi}$$

by the definitions of the Love numbers l_n and h_n . The surface strains are then

$$e_{\theta\theta} = \frac{1}{ga} \left(h_n V + l_n \frac{\partial^2 V}{\partial^2 \theta} \right)$$

$$e_{\phi\phi} = \frac{1}{ga} \left(h_n V + l_n \cot \theta \frac{\partial V}{\partial \theta} + \frac{l_n}{\sin \theta} \frac{\partial^2 V}{\partial^2 \phi} \right)$$

$$e_{\theta\phi} = \frac{l_n}{ga \sin \theta} \left(\frac{\partial^2 V}{\partial \theta \partial \phi} - \cot \theta \frac{\partial V}{\partial \phi} \right)$$

where the shear strain is tensor strain, not engineering strain. We next write the tidal potential, following equations (2.11) and (2.12), as

$$\frac{V}{g} = \sum_{n=2}^{n=\infty} \sum_{m=0}^m N_n^m P_n^m(\cos \theta) [a_n^m(t) \cos m\phi + b_n^m(t) \sin m\phi]$$

The following expressions then give the formulae for the three components of surface strain for a particular n and m ; to compute the total strain these should be summed over all $n \geq 2$ and all m from 0 to n (though in practice the tides with $n > 3$ or $m = 0$ are unobservable).

$$e_{\theta\theta} =$$

$$\frac{N_n^m}{a \sin^2 \theta} \left[\{h_n \sin^2 \theta + l_n(n^2 \cos^2 \theta - n)\} P_n^m(\cos \theta) - 2l_n(n-1)(n+m) \cos \theta P_{n-1}^m(\cos \theta) \right. \\ \left. + l_n(n+m)(n+m-1) P_{n-2}^m(\cos \theta) \right] \cdot \left[a_n^m(t) \cos m\phi + b_n^m(t) \sin m\phi \right]$$

$$e_{\phi\phi} =$$

$$\frac{N_n^m}{a \sin^2 \theta} \left[\{h_n \sin^2 \theta + l_n(n \cos^2 \theta - m^2)\} P_n^m(\cos \theta) - l_n(n+m) \cos \theta P_{n-1}^m(\cos \theta) \right] \\ \cdot \left[a_n^m(t) \cos m\phi + b_n^m(t) \sin m\phi \right]$$

$$e_{\theta\phi} =$$

$$\frac{m N_n^m l_n}{a \sin^2 \theta} \left[(n-1) \cos \theta P_n^m(\cos \theta) - (n+m) P_{n-1}^m(\cos \theta) \right] \cdot \left[b_n^m(t) \cos m\phi - a_n^m(t) \sin m\phi \right]$$

Note that the combination of the longitude factors with the $a_n^m(t)$ and $b_n^m(t)$ mean that $e_{\theta\theta}$ and $e_{\phi\phi}$ are in phase with the potential, while $e_{\theta\phi}$ is not.

It is useful to have explicit expressions for the largest tides, with $n = 2$ and $m = 1$ and 2 . Taking $a = 6.371 \times 10^6$ meters, the expressions for strain are:

$$n = 2 \quad m = 1:$$

$$e_{\theta\theta} = -2K(h_2 - 4l_2) \sin \theta \cos \theta [a_2^1(t) \cos \phi + b_2^1(t) \sin \phi]$$

$$e_{\phi\phi} = -2K(h_2 - 2l_2) \sin \theta \cos \theta [a_2^1(t) \cos \phi + b_2^1(t) \sin \phi]$$

$$e_{\theta\phi} = -2Kl_2 \sin \theta [a_2^1(t) \sin \phi - b_2^1(t) \cos \phi]$$

$$n = 2 \quad m = 2:$$

$$e_{\theta\theta} = K[h_2 \sin^2 \theta + l_2(4 \cos^2 \theta - 2)] \cdot [a_2^2(t) \cos 2\phi + b_2^2(t) \sin 2\phi]$$

$$e_{\phi\phi} = K[h_2 \sin^2 \theta + l_2(2 \cos^2 \theta - 4)] \cdot [a_2^2(t) \cos 2\phi + b_2^2(t) \sin 2\phi]$$

$$e_{\theta\phi} = -2Kl_2 \cos \theta [a_2^2(t) \sin 2\phi - b_2^2(t) \cos 2\phi]$$

where $K = 6.063 \times 10^{-8}$. The strain along a direction with azimuth ϕ (measured east from north) is

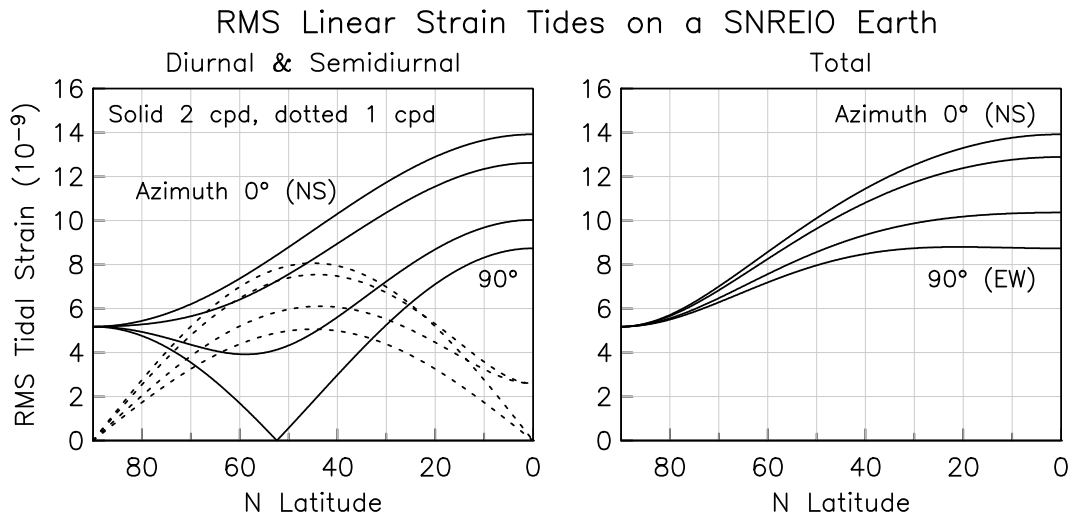
$$\varepsilon = e_{\theta\theta} \cos^2 \phi + e_{\phi\phi} \sin^2 \phi - 2e_{\theta\phi} \cos \phi \sin \phi$$

One consequence of these expressions is that the areal strain, $\frac{1}{2}(e_{\theta\theta} + e_{\phi\phi})$ is equal to $\frac{V}{ga}(h_2 - 3l_2)$: so for a SNREIO Earth, areal strain, vertical displacement, the potential, and gravity are all scaled versions of each other—as is volume strain, since for the tides the free-surface condition makes this a scaled version of areal strain.

Figure 6 shows the result of combining such a model with the known tidal forces, to show how the rms amplitude of the body tide in strain would vary with latitude on an elastic, oceanless earth. The left plot shows the rms tides in the two observable bands, for azimuths of 0° , 30° , 60° , and 90° : perhaps the most interesting feature is that the EW semidiurnal tides go to zero at 52.4° latitude. The tides are largest for the NS strain, and least for the EW. Tilt tides (not shown) are about four times larger than strain tides because they involve the direct attractions of the sun and moon; the purely deformational part is about the same size as the strain tide.

4. Tidal Loading

A large part of the difficulty in using earth tides to make inferences about the Earth lies in the signals caused by the ocean tides: a good example of one scientist's signals being another one's noise. The mass fluctuations associated with the ocean



tides would cause changes in the potential even on a rigid Earth, from the attraction of the water; on the real Earth they also cause the Earth to distort, which causes more change in the potential, plus displacements. All these make up the load tides, which are combined with the body tide to make up the total theoretical tide.

4.1. Basic Theory for Computing Loads

Given an ocean-tide model, the loads can be computed in two ways. One is to expand the tidal elevation in spherical harmonics; this is usually done for a particular constituent, with the tidal elevation being taken to be complex to express the amplitude and phase. We can write this expansion of the complex tidal elevation H as:

$$H(\theta, \phi) = \sum_{n=0}^{\infty} \sum_{m=-n}^n H_{nm} Y_{nm}(\theta, \phi) \quad (4.1)$$

where θ and ϕ , and Y_{nm} are as in the section on tidal forcing. Note that there are significant high-order spherical-harmonic terms in H_{nm} , if only because the tidal height goes to zero over land: any function with a step behavior will decay only gradually with increasing degree.

To compute the loads from this, we can use an expression such as, for the vertical displacement (for example)

$$\sum_{n=0}^{\infty} \sum_{m=-n}^n h'_n H_{nm} Y_{nm}(\theta, \phi) \quad (4.2)$$

or for the induced potential

$$\sum_{n=0}^{\infty} \sum_{m=-n}^n gk'_n H_{nm} Y_{nm}(\theta, \phi) \quad (4.3)$$

Here the h'_n and k'_n are called **load Love numbers**, since they are like the regular Love numbers, but are computed for a different boundary condition: the case in

which the surface of the Earth experiences a normal stress of given spherical harmonic degree, rather than this surface being a free surface and the interior experiencing a body force. For a spherical Earth these load numbers depend only on the degree n , not on the order m .

Many terms are needed for a sum in (4.2) or (4.3) to converge, but such a sum provides the complete displacement or potential over the whole Earth. If we only want the loads at a few places, a better method is to use a convolution. (There is a strict analogy with Fourier transforms: we may convolve two functions, or multiply their transforms.) The general convolution relation is an integral over the sphere (in practice over the oceans):

$$\int_0^\pi d\theta \int_0^{2\pi} d\phi G_L(\theta, \phi, \theta', \phi') \rho g H(\theta, \phi) \sin \theta \quad (4.4)$$

where G_L is the **Green function** for an effect (of whatever type) at θ', ϕ' from a point load (δ -function) applying a force of amount $\rho g H d\theta \sin \theta d\phi$ at θ, ϕ . For a spherically symmetric Earth, G_L will depend primarily on the angular distance Δ between θ, ϕ and θ', ϕ' , but not on their specific values. Given this independence of geographical coordinates, we can write (4.4) as an integral over distance Δ and azimuth θ from the location of an observation to the load:

$$\int_0^\pi d\Delta \int_0^{2\pi} d\theta G_L(\Delta, \theta) \rho g H(\Delta, \theta) \sin \Delta \quad (4.5)$$

where G_L depends on θ only through trigonometric expressions for vector or tensor quantities (tilt and strain).

This equation is the basis for most computations of ocean loads; to find it in practice we need:

- A. A description of H : that is to say, an **ocean-tide model**.
- B. Related to (A), a description of where the ocean ends: a **land-sea model**. Many ocean-tide models do not show this in much detail, so a supplementary representation is needed.
- C. A set of Green functions, for a specified SNREIO model and set of observables.
- D. Some software to combine all of these to compute (4.4) to adequate accuracy.

We consider each of these in turn.

4.2. Ocean and Land-Sea Models

Modeling ocean tides is an ancient subject, and a difficult one (Cartwright 1999). The intractability of the relevant equations (themselves put forward by Laplace in 1776) and the inability to measure tides in deep water meant that for a very long time there were no good tidal models for computing loads. From the Earth-tide standpoint what is important is that increasing computational power has finally rendered numerical solutions possible for realistic (complicated) geometries, and that satellite altimetry has provided a wealth of data with global coverage. For computing load tides, the ocean models are generally as good as they need to be.

Perhaps the biggest difficulty in modeling the tides is the need to represent the bathymetry in adequate detail (it is usually known adequately). The need to do this, and the relatively coarse spacing of the altimetry data, has meant that tidal models still divide into two groups: global and local. Global models often cannot adequately model the resonances that occur in some bodies of water (such as the Bay of Fundy), so local models must be used. Global models are computed on a relatively coarse mesh (say 0.5°), and rely heavily on altimetry data (e.g., Egbert and Erofeeva 2002). Local models use a finer mesh, and often rely on local tide-gauge data. Obviously, a local model is not important for computing loads unless you are close to the area it covers, but if you are it may be very important.

Most tidal models are given for particular tidal constituents, usually at least one diurnal and one semidiurnal. Unless a local resonance is present, the loads for other constituents can be found by scaling using the ratios of the amplitudes in the equilibrium tide. (Le Prevoist *et al.* 1991).

About land-sea models, little need be said: this problem has essentially been solved by the global coastal representations made available by Wessel and Smith (1996)—though these are not devoid of error, they will be adequate unless the station is very close to the shore, and the local tides are large. The only exception is in the Antarctic, where their coastline is (in places) the ice shelves, beneath which the tides are still present. The SPOTL software uses an improved coastline representation there.

4.3. Green Functions

The basic reference for tidal loading Green functions, and their computations, remains Farrell (1972); I give only a short sketch here. The Green functions are usually found as sums of load Love numbers, times the appropriate angular functions. For example, the Green function for vertical displacement is

$$G_z(\Delta) = \sum_{n=0}^{\infty} h'_n P_n(\cos \Delta)$$

where the P_n 's are the Legendre polynomials.

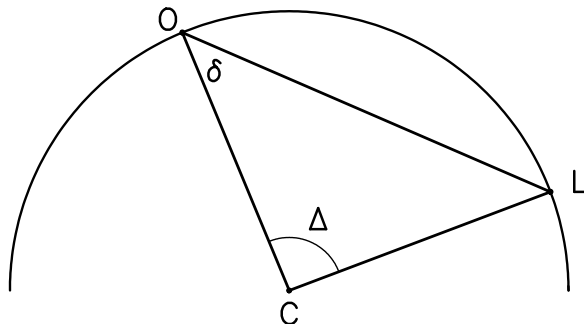


Figure 4.1

A few Green functions can be computed directly, notably the function for “Newtonian” (rigid-Earth or direct-attraction) gravity; finding this will illustrate some properties of such functions. The acceleration per unit mass is G/x^2 directed along

the line OL as shown in Figure 4.1; O is the place of observation, L of the load, and x the chord distance between them. The amount of acceleration directed along OC (the local vertical, to a good approximation) is

$$\frac{G \cos \delta}{x^2}$$

But $a \cos \Delta + x \cos \delta = a$, where a is the radius of the Earth, OC, so

$$\cos \delta = \frac{a(1 - \cos \Delta)}{x}$$

and also $x^2 = 2a^2(1 - \cos \Delta)$, so (11) becomes

$$\begin{aligned} \frac{G \cos \delta}{x^2} &= \frac{Ga(1 - \cos \Delta)}{2\sqrt{2} a^3 (1 - \cos \Delta)^{3/2}} \\ &= \frac{G}{2 a^2 \sqrt{2}(1 - \cos \Delta)} = \frac{G}{4 a^2 \sin \Delta/2} = \frac{g}{4M_E \sin \Delta/2} \end{aligned} \quad (4.6)$$

where M_\oplus is the mass of the Earth.

Note that this function has a singularity, of order Δ^{-1} , as Δ becomes small. Some kind of singularity at the origin is the general case, and shows that local loads are more important than distant ones: which is why local tidal models, and good representations of the shore, can be important. In reality, the response to gravity is not singular, in this case because of the effect of elevation above or below sea level (where the changes in mass occur).

The quantities for which Green functions are usually computed are displacement (vertical and horizontal), gravity, tilt, strain, and the tide-raising potential (a combination of potential change and vertical displacement). The Green function for linear strain, for example, is given by

$$G_L(\Delta, \theta) = G_\varepsilon(\Delta) \cos^2 \theta + \left[\frac{G_z(\Delta)}{a} + \cot \Delta \frac{G_h(\Delta)}{a} \right] \sin^2 \theta \quad (4.7)$$

where θ is the azimuth of the load relative to the direction of extension, and G_ε , G_z , and G_h are the Green functions for strain in the direction of the load, and vertical and horizontal (toward the load) displacement.

For small distances, the Green functions for displacement, gravity, and the potential vary as Δ^{-1} , and tilt and most kinds of strain as Δ^{-2} . Areal strain has a complicated dependence on distance, because it in fact is zero for a point load on a halfspace, except right at the load. The singularity in strain again is removed in practice by any depth of burial. The higher order of singularity for tilt and strain means that the computed ocean load, especially near a coast, can be dominated by local tides.

Green functions were computed by Farrell for three earth models: one average, one with a continental structure, and one with an oceanic structure. The differences were not large. Later authors (e.g., Jentzsch 1997) have computed these functions for more modern models (eg PREM), and also for other depths than at the surface (to look at tidal triggering). Examination of the extent to which local structure,

particularly lateral variations, affect computed load tides, have not be plentiful—perhaps mostly because the data most sensitive to such effects, strain and tilt, are affected by other local distortions.

4.4. Computational Methods

Essentially all load programs perform the convolution (4.4) directly, either over the grid of ocean cells (perhaps subdivided near the load) or over a radial grid. Bos and Baker (2005) have recently compared the results from four programs, albeit only for gravity, which is least sensitive to local loads. The programs included SPOTL and GOTIC, the only two that compute strain loads. They find variations of a few percent because of different computational assumptions.

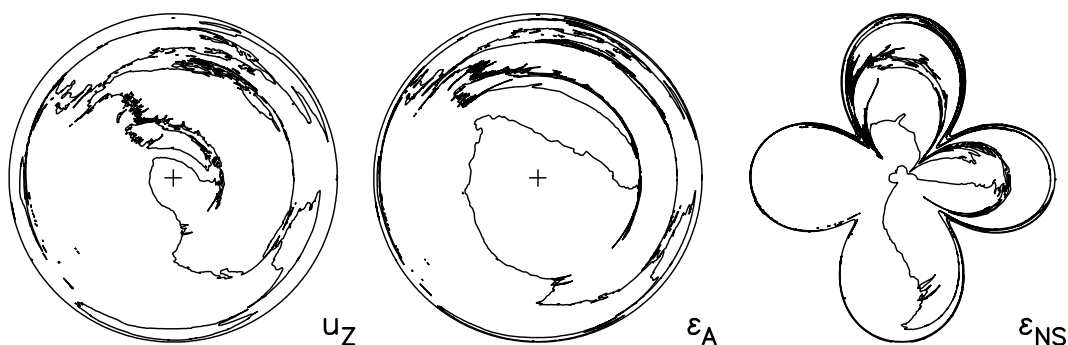


Figure 4.2

4.5. An Example

To show how this works in practice, we consider the PBO borehole strainmeter (and GPS site) HOKO, on the Olympic Peninsula in Washington. We first show a set of maps (Figure 4.2) in which areas are deliberately distorted so that regions of equal area on the map would contribute equally to the measurement if the loads on them were the same (Agnew 2001). Such a map immediately shows which regions of loading are unimportant, and which are possibly significant, though of course the actual significance of any area depends on there actually being a load there. The map is thus how a measurement at some place “views” the world of loads, Figure 4.2 shows such maps for vertical displacement (important for GPS), areal strain, and NS strain. The first two are both independent of azimuth; the last is insensitive to loads at 45° to the NS axis, producing a 4-lobed pattern. For the displacement, the North Pacific occupies most of the area on the map. For the strain, the greater localization of the Green function is shown by the much greater prominence of the Strait of Juan de Fuca. Accurate calculation of these loads thus demands good local tide models, an accurate depiction of the coastline, and Green functions that represent the local structure. While detailed local models for many of the of the world’s coasts do not yet exist, this is not true here.

Figure 4.3 shows what the actual computation produces, in the standard form of a phasor plot (phase lags negative, and relative to the local potential). The Green function is Farrell’s for the Gutenberg-Bullen average model. In each frame, the first arrow is the M_2 tide expected on a SNREIO Earth: large for the NS extension,

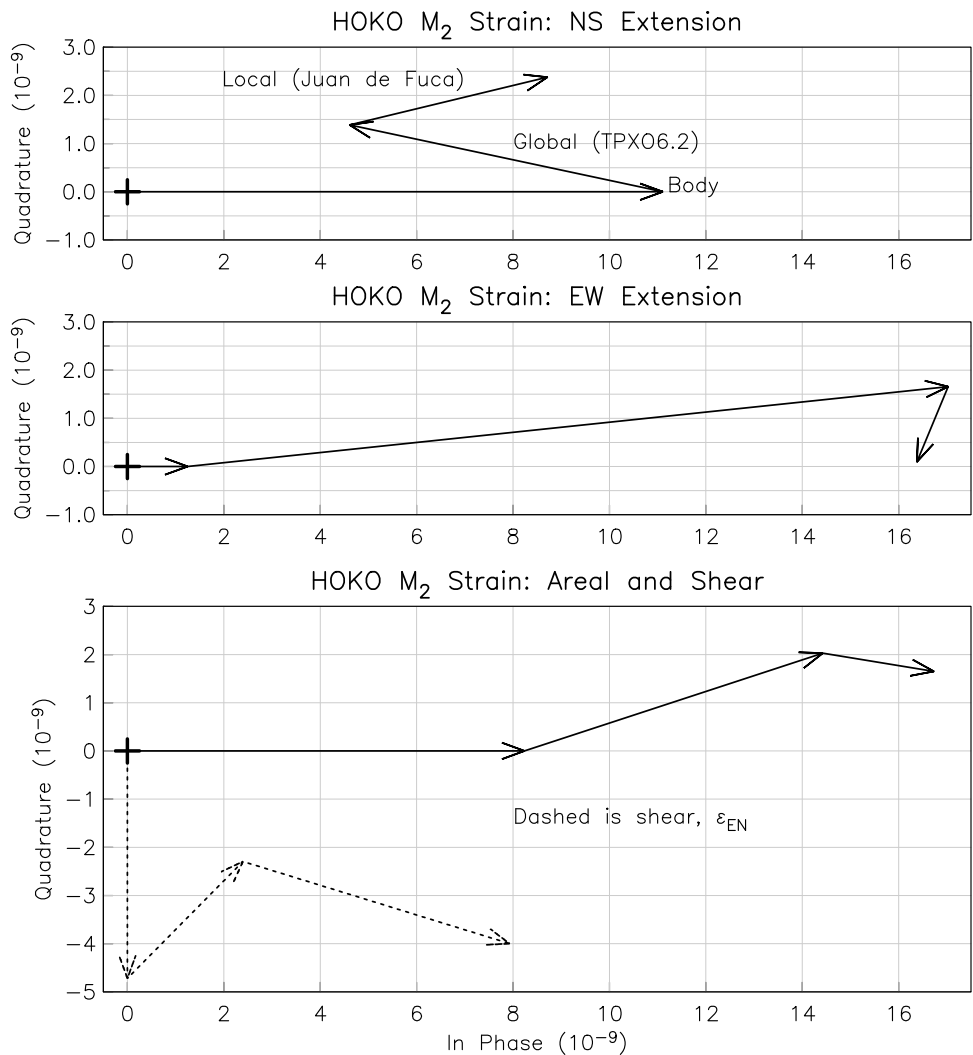


Figure 4.3

very small for the EW, and in quadrature (90° phase) for the shear. The loads modify this signal very substantially, greatly increasing the amplitude of the EW but not much changing the phase (not true in general), and changing the amplitude and phase of the shear. The local tides in the Strait of Juan de Fuca are important but not dominant; what probably dominates are the Pacific Ocean tides nearby, which are fairly well known. Using a continental structure changes the EW tide by about 10%. Clearly, getting the loads right, at this site, will be important, but not extremely difficult.

5. Tidal Analysis and Prediction

We close our discussion of tides with the analysis of time series for tidal response, and the prediction of future tides from such an analysis. To start with, we note that what we are really are trying to determine is the response of some system to the tidal forcing. The relevant concept is therefore that of the admittance of a linear system, first introduced into tidal analysis by Munk and Cartwright (1966). We

suppose that our data $y(t)$ can be represented as, for example,

$$y(t) = \int x_T(t - \tau) h_T(\tau) d\tau + \int x_B(t - \tau) h_B(\tau) d\tau + n(t) \quad (4.1)$$

Here the $x(t)$'s are input series: x_T is a theoretical tide, and x_B is (say) the local air pressure; there might be more series for other environmental variables as well. The function $n(t)$ is the noise—which in this representation simply means “anything not correlated with the input series”; it may include, along with instrument drift, and short-term noise, such things as tectonic changes (which are noise if you are interested in tides).

The functions $h(t)$ then give the impulse response of the system to the various inputs. If we take the Fourier transform of both sides of (4.1), and disregard the noise, we find that $Y(f) = H_T(f) X_T(f) + H_B(f) X_B(f)$. The $H(f)$'s are **admittances**, the Fourier transforms of the h 's—and it is, almost always, more informative to examine these frequency-domain functions than their time-domain counterparts. If $x_T(t)$ is the tidal potential, it may be computed from known astronomy to a level that we may regard as exact. Because the tides are very band-limited we can find the **tidal admittance**, $H_T(f)$, only for frequencies at which $X_T(f)$ contains significant energy—so it is not really feasible to determine $h(t)$. In studying ocean tides it is most meaningful to take $x_T(t)$ to be the local value of the tide-raising potential. In earth tide studies it may be more convenient to take as reference the tides expected for a SNREIO earth model, so that any departure of $H(f)$ from unity will then reflect the effect of ocean loads or the inadequacy of the model.

5.1. The Credo of Smoothness

Thinking about the tides in terms of the admittance leads to an important insight that is implicit in some methods of tidal analysis and explicit in others. This is that the admittance is a smoothly-varying function of frequency, so that, over each of the tidal bands $h(f)$ does not vary a great deal—and, the more closely spaced two frequencies are, the closer the corresponding values of $h(f)$ will be. This assumes that neither the ocean nor the Earth have resonant responses in the tidal bands, at least not sharp ones, which is to say ones with a very high Q . Munk and Cartwright (1966) dubbed this assumption “the credo of smoothness”.

This assumption appears to be valid and useful for the response of the ocean: even though there are many modes of oscillation with frequencies in the tidal bands, most of them have such low Q 's as to be undetectable. Even the local resonances in certain bays and gulfs have a low enough Q that the response is smoothly-varying over (say) the complete semidiurnal band. The one place where this assumption breaks down is in the Free Core Nutation resonance in the Love numbers (Section 3.0 above), though this is small enough to (usually) be ignored in tidal analysis schemes.

5.2. Tidal Phase Conventions

A frequent source of confusion in using the results of a tidal analysis is what the phases mean. First of all, there is a sign issue; namely which sign of phase represents a lag (or lead). At bottom this comes down to what our Fourier transform

convention is, or, put another way, what we use to represent a complex sinusoid. If this is $e^{2\pi i(ft + \phi)}$, then for $\phi = 0$, the maximum will occur at $t = 0$. If ϕ is (slightly) greater than 0, the maximum will be at $t < 0$, and the function will be advanced (we reach the maximum sooner in time) relative to $\phi = 0$; similarly for $\phi < 0$, we reach the maximum later (a delay). Thus, $\phi < 0$ is a phase lag, and $\phi > 0$ a phase lead. This corresponds to using $e^{-2\pi if t}$ as the kernel in the definition of the Fourier transform. This is the choice used in electrical engineering (and hence in signal processing), and becoming increasingly common. However, much of the tidal literature reflects the more common convention of the nineteenth century, which is to make phase lags positive.

This is a problem for any Fourier results; one peculiar to tidal analysis is, what do we refer the phases to? Otherwise put, when is the phase zero? There are two common choices:

1. The **local phase**, in which the phase is taken to be zero (for each constituent) at a time at which the potential would be a maximum, locally. This is a convenient choice for the analysis of Earth tides because on a SNREIO Earth the phase is zero for most tides (e.g., gravity, NS tilt, vertical displacement, areal strain). For ocean tides this phase is usually denoted as κ , though note that in this field that variable refers to positive phases for lags. For strain in an arbitrary direction, the local phase varies in a more complicated way. We can of course choose the reference to be when the phase of the corresponding theoretical tide (e.g., linear strain in the same direction on an SNREIO Earth) is zero, though this is not a standard choice.
2. The **Greenwich phase**, in which the phase is taken to be zero (for each constituent) at a time at which the potential would be a maximum at 0° longitude. The purpose to this is that, if given for a number of places, it provides a “snapshot” of the distribution of the tidal amplitude and phase at a particular instant. This phase, usually termed G , is therefore the norm in ocean-tide studies;⁷ again usually with lags positive.

The relationship between κ and G is simple, and depends only on the tidal species number m and the longitude L since the time between maximum at Greenwich and maximum at a local place depends only on the spherical harmonic order (and the Earth rotating 360° every 24 hours): the frequency of the constituent is not involved. The relationship is usually written as

$$G = \kappa - mL$$

Note however, that this not only assumes phase lags to be positive, but West longitudes to be positive as well: an old convention of diminishing popularity. If we use primes on G and κ to denote lags negative, and take East longitudes (λ) to be positive (now the more common choice), we get what looks like the same rule:

$$G' = \kappa' - m\lambda \tag{4.2}$$

It is obviously very important, when using or giving the results of a tidal analysis, to

⁷ Not completely true; many collections of tidal constants use another phase, g , which is the phase corrected to local time—as makes sense if you want to predict tides for a particular port.

be explicit about the phase conventions being used.

5.3. Preprocessing Data for Tidal Analysis

All tidal analysis is an attempt to extract information from a few relatively narrow frequency bands. An ideal series for tidal analysis would be one with no noise at all; and while this is not possible, it is useful to try to make it as good an approximation as can be done. In particular, if there is considerably more energy present in the series at frequencies away from the tides, than at frequencies nearby, it is a good idea to remove this energy before performing the analysis. Many series that contain tidal data, and borehole strainmeter data most of all, have much more energy at low frequencies (in the form of drift) than in the tidal bands. Because the only goal for tidal preprocessing is to remove energy in some frequency bands, this drift can be most easily removed by convolving the series with an appropriate high-pass filter. If a zero-phase-shift FIR filter is used, the only correction then needed is (perhaps) for the tidal amplitudes to be modified for the filter response, though it is not difficult to design filters with negligible departure from unity gain in the pass-band.

5.4. Spectral and Cross-Spectral Methods

The most naive approach to finding the tidal response is to simply take the Fourier transform of the data, and look at the amplitudes and phases of the result. That is, given N data values y_n , we compute the Discrete Fourier Transform (DFT) coefficients

$$Y_k = \sum_{n=0}^{N-1} y_n e^{-2\pi i n k / N} \quad k = 0, \dots, N-1 \quad (4.3)$$

and use their amplitudes and phases to get the amplitudes and phases of the tides. This is a really bad choice, made even worse if the length of the transform, N is made to be a power of 2 to utilize a Fast Fourier Transform algorithm. There are (at least) two problems with this:

- A. The frequencies corresponding to the indices k for the DFT coefficients are $f_k = k/N\Delta t$, where Δt is the sample interval. These may or may not coincide with the frequencies of the tidal constituents—and usually they do not.
- B. The amplitudes of the coefficients will be biased to values higher than the true values because of the presence of noise, the limiting case being that $|Y_k|$ will have some positive value even if there is no tidal signal at all.

A much better method, still based on spectral techniques, is the cross-spectral technique described by Munk and Cartwright (1966). While this method has lower frequency resolution than some others, it makes the fewest assumptions about the data being analyzed, and in particular about the form of $H(f)$. Another advantage is that it allows the noise to be determined as a function of frequency, whereas most methods assume it to be the same at all frequencies. This may not be true for strain data. As the method was described in full by Munk and Cartwright I give only a brief summary.

The procedure is to compare the data series y with a computed series of theoretical tides x , which is of course noise-free.⁸ Then divide each series into M sections of length N , and compute an array of DFT coefficients for each series:

$$X_{lm} = \sum_{n=0}^{N-1} W_n X_{n+j(m)} e^{-2\pi i l n / N} \quad (4.4a)$$

$$Y_{lm} = \sum_{n=0}^{N-1} W_n Y_{n+j(m)} e^{-2\pi i l n / N} \quad (4.4b)$$

where $j(m)$ is the starting term of the m -th section. If there are no gaps to skip over, $j(m) = (m-l)r$, where r is the offset between successive sections. The value of M will of course depend on r , on the total length of the series, N , and on the distribution of gaps. The sequence W_n is termed a **window**, or **data taper**, used on the data before Fourier transforming; it serves to minimize bias of small signals by large ones nearby in frequency.

In order to compute cross-spectral estimates, we must average the Fourier transforms—if we just take a single pair of DFT coefficients, we will get a badly biased answer. Two ways of proceeding, which may be combined, are averaging over sections and averaging over frequency. (The reason for frequency averaging rather than using shorter sections is that certain section lengths minimize the sidebands from the tidal lines.) Suppose we are interested in the cross-spectrum at a frequency bin l_1 , where $l_0 < l_1 < l_0 + L - 1$. Denote the summation process by

$$S[Z] = \sum_{l=l_0}^{l_0+L-1} \sum_{m=1}^M Z_{lm}$$

The estimated admittance is then

$$\hat{H} = \frac{S[X^* Y]}{S[X^* X]} \quad (4.5)$$

The input and output power spectral densities are

$$\hat{P}_i = \frac{S[X^* X]}{LMN_W} \quad \hat{P}_0 = \frac{S[Y^* Y]}{LMN_W} \quad (4.6)$$

where N_W is the normalizing factor for the window W :

$$N_W = \sum_{n=0}^{N-1} W_n^2$$

The estimated coherence between the series is

$$\hat{\gamma}^2 = \frac{\left(S[\operatorname{Re}(X^* Y)] \right)^2 + \left(S[\operatorname{Im}(X^* Y)] \right)^2}{S[X^* X] S[Y^* Y]} \quad (4.7)$$

⁸ This can be computed from the methods described in Section 2 and Section 3, either to compute the potential or to compute a theoretical tide on a SNREIO Earth.

Munk and Cartwright (1966) show that the coherence estimated from a finite record will be biased high; an approximately unbiased estimate of the coherence is

$$\gamma^2 = \frac{p \hat{\gamma}^2 - 1}{p - 1} \quad (4.8)$$

Here p depends on the amount of averaging; if the estimates from each segment are independent it is ML . The number of degrees of freedom (in the statistical sense) is $2p$. The admittance estimate \hat{H} is complex; Munk and Cartwright give the probability distribution for the amplitude and phase of H . If the signal-to-noise ratio is high, both are distributed nearly normally with variance

$$\sigma^2 = \frac{\gamma^{-2} - 1}{2p} \approx \frac{1 - \hat{\gamma}^2}{2p} \quad (4.9)$$

for $p \hat{\gamma}^2 \gg 1$. Finally, the noise power is given by

$$P_N = P_0(1 - \gamma^2) \quad (4.10)$$

A reasonable procedure is to first lowpass and decimate the data to a 3 hour interval. Putting $N = 1093$ then gives a record length of almost exactly 132 lunar days or 4 lunar months, which ensures that the tidal groups all fall close to integral frequencies of the digital Fourier transform. Application of a Hanning window to the data ensures that the tidal energy in each group is confined to only three frequencies. Averaging over these when computing the cross-spectrum gives a final frequency resolution of 1 cycle per month. If the data sections are overlapped by 50 percent, the appropriate value for p was $1.4LT/N$, where T is the total length of the series (Haubrich 1965).

The program `tidspec` implements this analysis procedure, using a slow Fourier transform algorithm to compute the (relatively few) DFT coefficients needed, without the length restrictions of an FFT. This takes care of objection (A) above; objection (B) is removed by the averaging and use of cross-spectral estimation. Again, this method makes few assumptions and provides estimates of the noise spectrum; it does however require large amounts of data (at least a few years) to perform reliably.

5.5. Least-squares Fitting

By far the most common approach to tidal analysis, is least-squares fitting of a set of sinusoids with known frequencies—chosen, of course, to match the frequencies of the largest tidal constituents. It is easy to set this up; we aim to minimize the sum of squares of residuals r_n , formed by

$$\sum_{n=0}^N \left[y_n - \sum_{l=1}^L \left(A_l \cos(2\pi f_l t_n) + B_l \sin(2\pi f_l t_n) \right) \right]^2 \quad (4.11)$$

which expresses the fitting of L sine-cosine pairs with frequencies f_l to the data, the f 's being fixed and the A 's and B 's being solved for.⁹

⁹ Fitting for amplitudes and phases, being a nonlinear problem, should never be done.

The mathematics for solving such a problem are quite standard, though the usual assumption for the noise (that it is independent for each sample) is probably not valid in this case. One minor point about the least-squares solution is that it can be solved using the normal-equations version of the associated matrix problem. Because of numerical instabilities in forming the normal equations, least-squares problems are usually better solved using other matrix methods such as singular value decomposition; in this case the normal equations involve sums of sines and cosines, and these can be found analytically.

The problem with using (4.11) for tidal analysis comes from the fine-scale frequency structure of the tidal forcing function, particularly the nodal modulations. Leaving such variations out of (4.11), and only solving for a few large constituents, will in general be quite inaccurate. But the simplest way of including nodal and other modulations, namely through including the satellite constituents in (4.11), will not work because (unless we have 19 years of data) we will be trying to solve for the amplitudes of constituents separated by frequency by less than $1/T$, where T is the record length: and this cannot be done reliably.¹⁰ This is a problem for other tides if we have only a short span of data: for example, with only a month of data, we cannot get reliable results for the P_1 and K_1 lines, since they are separated by only 0.15 cycles/month.

All least-squares analysis procedures thus have to include an assumption about nearby tidal constituents, which is to say an implicit assumption about the admittance. The usual one is to take the admittance to be constant over widths $1/T$ around the main constituents, summing all constituents within each such group to form (slowly varying) sinusoidal functions to replace the sines and cosines of (4.11). This is, for example, the procedure in BAYTAP. Of course, if we then wish to assign the resulting amplitude to a particular constituent (say M_2) we need to correct the amplitudes solved for by the ratio of this sinusoidal function to the single constituent. All this adds complexity; while it has been taken care of in existing analysis programs, it would need to be implemented in any new one.

5.6. The Response Method

One way of avoiding these complications, and perhaps the most sophisticated approach to tidal analysis, is the **response method** introduced by Munk and Cartwright (1966). This makes no use at all of the harmonic expansion of the tidal potential, but rather treats this as a time series to be fit to the data, using a set of weights to express the admittance. Except for Lambert (1974) it has not been much applied to Earth tide analysis, in large part (in my view) because of an overly-conservative attachment to being able to give amplitudes of coefficients. It also has not seen much use in the analysis of ocean-tide data, with the very notable exception of the estimation of tides from satellite altimetry, where it is standard.

The basic approach is a weighted sum over the time variations by spherical harmonic (*not* harmonics in time):

¹⁰ This limit is known as Rayleigh's criterion. It actually depends (somewhat) on the signal to noise level.

$$y(t) = \sum_{n=2}^{\infty} \sum_{m=-n}^n \sum_{l=-L_{nm}}^{L_{nm}} w_{nl}^m [a_n^m(t - l\Delta) + ib_n^m(t - l\Delta)] \quad (4.12)$$

where the $a_n^m(t)$ and $b_n^m(t)$ are the time-varying functions that sum to give the potential in (2.11). The (complex) weights w_{nl}^m , called **response weights**, give the tidal response; to get this as a function of frequency we would take the Fourier transform of the series of weights. Taking one weight for each n and m (that is, setting $L_{nm} = 0$) amounts to assuming a constant admittance for each degree and order. Note that because even one weight would be complex, it can express both amplitude and phase response. Including more weights, with lags, allows the admittance to vary with frequency, smoothly, across each tidal band. The lag interval is usually chosen to be 2 days, which makes the admittance smooth over frequencies of greater than 0.5 cpd; note that the lags can include the potential at future times because the admittance is being fit over only a narrow frequency band.

5.7. Predicting Tides

All tidal predictions, other than those based on the response method, use a harmonic expansion similar to equation (2.13):

$$x(t) = \sum_{k=1}^K A_k \cos \left[2\pi f_k(t - t_0) + \phi_k^0(t_0) + \phi_k \right] \quad (4.13)$$

where the A_k 's and ϕ_k 's are amplitudes and phases (the **harmonic constants**) for whatever is being predicted. The f_k 's are the frequencies of the different constituents, and the ϕ_k^0 's are the phases of these at a reference time t_0 .

This much is straightforward; the complications come from the various long-term modulations of the tides, as for example the nodal modulations discussed in Section 2.5. In classical prediction methods, these are applied to adjust the various A_k 's and ϕ_k 's so as to produce gradually changing values, after which a sum was done over a relatively small number of constituents.¹¹ This works perfectly well, but adds complexity, especially if the predictions are to be made over a long time, during which these adjustments will change.

There is a conceptually simpler approach, though since it is more computationally intensive, it was not usable until modern computers were available. This is to simply use a large number of constituents in a sum of the form (4.13) with satellite constituents being included to produce the nodal and other modulations. The problem then is to infer the amplitudes and phases of these, since they usually cannot be analyzed for. The method (implicit in the classical method as well) is to rely on the smoothness of the tidal admittance, and use this to find the amplitudes and phases of many constituents from those few that are available. This procedure is implemented in the program `hartid`, using a spline interpolation of the real and imaginary parts of the admittance, which is itself deduced by taking the ratio of constituent amplitudes to those amplitudes for the equilibrium potential, using the

¹¹ Another of Thomson's contributions to tidal methods was the mechanical tide prediction machine, which used geared cranks to produce the sinusoids and a long belt connecting them to make the sums. These analog systems were in fact faster than the early digital computers, and were not replaced by them until the 1960's.

values for the CTED expansion. (See Le Prevost *et al.* 1991, for a description, though `hartid` was developed independently of this work).

References

- D. C. Agnew, "Map projections to show the possible effects of surface loading," *J. Geodetic Soc. Japan*, 47, pp. 255-260 (2001).
- M. S. Bos and T. F. Baker, "An estimate of the errors in gravity ocean tide loading computations," *J. Geodesy*, 79, pp. 50-63 (2005).
- R. A. Broucke, W. Zurn, and L. B. Slichter, "Lunar tidal acceleration on a rigid Earth," *AGU Geophys. Monogr.*, 16, pp. 319-324 (1972).
- Stephen G. Brush, *Nebulous Earth: the Origin of the Solar System and the Core of the Earth from Laplace to Jeffreys*, Cambridge University Press, Cambridge (1996).
- F.-J. Bullesfeld, "Ein Beitrag Zur Harmonischen Darstellung Des Gezeitenerzeugenden Potentials.," *Deutsche Geod. Komm., Reihe C.*, 31, pp. 3-103 (1985).
- D.E. Cartwright and A.C. Edden, "Corrected tables of tidal harmonics," *Geophys. J. Roy. Astron. Soc.*, 33, pp. 253-264 (1973).
- D.E. Cartwright and R.J. Tayler, "New computations of the tide-generating potential," *Geophys. J. Roy. Astron. Soc.*, 23, pp. 45-74 (1971).
- David E. Cartwright, *Tides: a Scientific History*, Cambridge University Press, New York (1999).
- A. T. Doodson, "The harmonic development of the tide generating potential," *Proc. Roy. Soc. Ser. A*, 100, pp. 305-329 (1921).
- G. D. Egbert and S. Y. Erofeeva, "Efficient inverse modeling of barotropic ocean tides," *J. Atmosph. Oceanic Tech.*, 19, pp. 183-204. (2002).
- W. E. Farrell, "Deformation of the earth by surface loads," *Rev. Geophys.*, 10, p. 761-797 (1972).
- J. C. Harrison, "New Programs for the Computation of Earth Tides," CIRES, University of Colorado (1971).
- J. C. Harrison, *Earth Tides*, Van Nostrand Reinhold, New York (1985).
- T. Hartmann and H.-G. Wenzel, "The HW95 tidal potential catalogue," *Geophys. Res. Lett.*, 22, pp. 3553-3556 (1995).
- R.A. Haubrich, "Earth noise, 5 to 500 millicycles per second 1. spectral stationarity, normality and nonlinearity," *J. Geophys. Res.*, 79, pp. 1415-1427 (1965).
- G. Jentzsch, "Earth tides and Ocean tidal loading" in *Tidal Phenomena*, ed. H. Wilhelm, W. Zürn, and H. G. Wenzel, pp. 145-171, Springer-Verlag, Berlin (1997).
- S. M. Kudryavtsev, "Improved harmonic development of the Earth tide-generating potential," *J. Geodesy*, 77, pp. 829-838 (2004).
- A. Lambert, "Earth tide analysis and prediction by the response method," *J. Geophys. Res.*, 79, pp. 4952-4960 (1974).

- C. LePrevost, F. Lyard, and J. Molines, "Improving ocean tide predictions by using additional semidiurnal constituents from spline interpolation in the frequency domain," *Geophys. Res. Lett.*, 18, pp. 845-848 (1991).
- I. M. Longman, "Formulas for computing the tidal accelerations due to the Moon and the Sun," *J. Geophys. Res.*, 64, pp. 2351-2355 (1959).
- P. Melchior, *The Tides of the Planet Earth*, Pergamon, New York (1983).
- J. B. Merriam, "An ephemeris for gravity tide predictions at the nanogal level," *Geophys. J. Int.*, 108, pp. 415-422 (1992).
- W.H. Munk and D.E. Cartwright, "Tidal spectroscopy and prediction," *Phil. Trans. Roy. Soc., Ser. A.*, 259, pp. 533-581 (1966).
- F. Roosbeek and 1995, "RATGP95: a harmonic development of the tide-generating potential using an analytical method," *Geophys. J. Int.*, 126, pp. 197-204.
- Y. Tamura, "A harmonic development of the tide-generating potential," *Bulletin d'Informations Marees Terrestres*, 99, pp. 6813-6855 (1987).
- P. Wessel and W. H. F. Smith, "A global, self-consistent, hierarchical, high-resolution shoreline database," *J. Geophys. Res.*, 101, pp. 8741-8743 (1996).
- H. Wilhelm, W. Zürn, and H. G. Wenzel, *Tidal Phenomena*, Springer-Verlag, Berlin (1997).
- Qinwen Xi, "A new complete development of the tide-generating potential for the epoch J2000.0.," *Bulletin d'Informations Marees Terrestres*, 99, pp. 6766-6812 (1987).